CONF-871024--8

. **LA-UR** -87-2082

Los Alamos National Laboratory is operated by the University of California for the United States Department of Energy under contract W-7405-ENG-36

LA-UR--87-2082

DE87 011765

TITLE Identification of MHF Fracture Planes and Flow Paths by Correlating Well Log Data with Patterns in Locations of Induced Seismicity

AUTHOR(S) Don Dreesen
Mark Malzahn
Michael Fehler
Zora Dash

SUBMITTED TO Geothermal Resources Council

DISCLAIMER

Los Alamos National Laboratory
Los Alamos, New Mexico 87545

DISCLAIMER

IDENTIFICATION OF MHF FRACTURE PLANES AND FLOW PATHS: A CORRELATION OF WELL LOG DATA WITH PATTERNS IN LOCATIONS OF INDUCED SEISMICITY

Don Dreesen, Mark Malzahn*, Mike Fehler, Zora Dash

Los Alamos National Laboratory, P.O. Box 1663, MS J981, Los Alamos, New Mexico 87545
*Consultant, P.O. Box 1663, MS J981, Los Alamos, New Mexico 87545

ABSTRACT

One of the critical steps in developing a hot dry rock geothermal system is the creation of flow paths through the rock between two wellbores. To date, circulation systems have only been created by drilling one wellbore, hydraulically fracturing the well (which induces microearthquakes), locating the microearthquakes and then drilling a second wellbore through the zone of seismicity. A technique for analyzing the pattern of seismicity to determine where fracture planes are located in the seismically active region has recently been deveolped. This allows us to distinguish portions of the seismically active volume which are most likely to contain significant flow paths. We applied this technique to seismic data collected during a massive hydraulic fracturing (MHF) treatment and found that the fracture planes determined by the seismic method are confirmed by borehole temperature and caliper logs which indicate where permeable fractures and/or zones of weakness intersect the wellbores. A geometric model based on these planes and well log data has enhanced our understanding of the reservoir flow paths created by fracturing and is consistent with results obtained during production testing of the reservoir.

INTRODUCTION

The use of microearthquake locations to accurately locate hydraulic fractures is an essential step in the development of Hot Dry Rock (HDR) technology. During the course of the DOE Fenton Hill Hot Dry Rock Geothermal Energy Program, considerable effort has been made in evaluating seismicity as a means of determining where fluid has penetrated the geothermal reservoir during hydraulic injections (Albright and Hanold, 1986; Pearson, 1981; House et al., 1985). During phase II of the HDR project, we have conducted many injections into wellbores EE-2, EE-3 and EE-3A to fracture various regions of the potential geothermal reservoir. Some of these experiments are described in Table 1. Of particular importance was a 21,600 m^3 injection into wellbore EE-2, called Exp 2032, which induced a large number of microearthquakes. We located many of these microearthquakes (House et al., 1985, House, 1987) and used the density of locations to select a trajectory for wellbore EE-3A which, when drilled was found to penetrate hydraulically-created fractures (Dreesen et al., 1985).

Injections into various intervals of EE-3A where the well penetrated the zone of seismicity induced by Exp 2032 yielded inconsistent results in obtaining hydraulic communication with EE-2. This demonstrated that the reservoir is complex and cannot be simply modeled as a volumetrically distributed, highly fractured reservoir throughout the region occupied by the microearthquake locations. Knowledge only of regions with high seismicity is insufficient to guarantee that a flow path will be encountered during drilling. Thus, techniques that define flow paths and model the reservoir structure are needed.

Fehler et al. (1987) developed the three point method to determine the locations and orientations of planes along which microearthquakes occurred, hence finding likely flow paths. They applied the method to locations of microseismic events accompanying Exp 2032 and found planes with five unique orientations. In order to lend further credibility to the method, it is important to correlate the locations of these planes with other data from the reservoir. In this paper, we describe the correlation of the positions of these five planes with wellbore temperature anomalies, indicating where fracture zones intersect wellbores (Murphy, 1982), and caliper anomalies which indicate where zones of weakness intersect wellbores.

The three point method is a three-dimensional extension of a two-dimensional procedure developed by Lutz (1986). The method, along with tests to demonstrate its validity, are described in detail by Fehler et al., (1987) so only a brief description will be given here. To apply the method, all microearthquake locations are taken three at a time in order to determine orientations (strike and dip) of all possible planes in the data set. The range of all possible orientations is divided into subsets of similar (e.g. ±2°) orientations and the number of planes within each subset is counted and corrected for a shape bias. The subset with the greatest number of three-point solutions gives the general orientation of the dominant plane, and the microearthquakes that contribute to this subset are identified. A preliminary location of the plane is determined by plotting the locations of these microearthquakes. Additional planes can be found by removing the events that occur along the planes given by previous solutions and reapplying the method.

Fehler (1987) has applied the three point method to locations of microseismic events accompanying four hydraulic injections into the Fenton Hill reservoir. His results led him to conclude that the microseismic events that accompany water injections into crystalline rock are caused by shear slip along pre-existing joints or planes of weakness in the rock. We infer these to be the dominant paths for fluid flow. The seismically active portions of the planes are significant because the effective stresses have changed enough in these regions to cause slip to occur. This change in stress is associated with the presence of pressurized fluid. The extent of the zone of weakness to regions beyond the seismically active portion of a plane is uncertain. However, it is possible that this zone extends beyond the seismically active portion, but that microearthquakes did not occur in these regions because of variations in mechanical properties of the rock or because the fluid that penetrated beyond the seismically active region was of insufficient pressure to induce seismicity.

RESULTS OF THE THREE POINT METHOD

The three point method was applied to a dataset consisting of 844 locations of microearthquakes accompanying Exp 2032, approximately 5% of the locatable microearthquakes recorded during the injection. The five planes associated with Exp 2032 all passed the statistical significance test that there be a less than 1 in 10000 probability of being identified by chance. These planes contained 38% (324) of the Exp 2032 locations. A least-squares determination (Schomaker et al., 1959) of the best fit to the locations that fell about each plane was used to refine each plane's orientation. The planes thus determined were identified with a number to represent the order in which they were found by application of the three point method (the lower the number, the greater the statistical significance of the plane).

Histograms of the number of microearthquakes as a function of their perpendicular distance from their best-fit plane were generated. In some cases, the histogram contained well defined peaks (see Figure 1). If the peaks in the distribution were separated by greater than 20 m, roughly the relative uncertainty in microearthquake locations (House, 1987), we assumed that each peak represented one plane and further segregated the locations. The orientations of the resulting planes were then determined using the least-squares method. If multiple planes with similar or equivalent orientations were found, a letter was placed next to the plane number.

COMPARISON OF THREE-POINT RESULTS WITH TEMPERATURE AND BOREHOLE CALIPER LOGS

After the planes were identified, the depth where each plane intercepted each wellbore was calculated. Table II lists all of the planes found by three point analysis of the Exp 2032 microearthquake locations and the intercept depths. The correlation of these intercepts with fluid injection zones (as determined from temperature logs) and/or with zones of weakness (as determined from caliper log breakout zones) are also described. In addition, the typical surface fluid injection pressure for each injection interval is listed. We also indicate whether the intersection between the wellbore and the plane occurs in a seismically active portion of the plane or extension of the plane beyond the seismically active zone. The angle between the plane and wellbore is given since the length of intersection between the plane and borehole has greater uncertainty for low angle intercepts due to uncertainties in borehole and microearthquake locations. In addition, low angle intercepts may result in a longer zone of disturbance in the borehole logs due to a longer portion of the wellbore being in close proximity to the fracture. We will now describe in detail a few of the relationships between the well logs and the seismic plane intercepts.

Injection Zone Intercepts in EE-2

Planes 1 and 5A intersect borehole EE-2 in the interval, from 3530 to 3658 m, where water was first injected during Exp 2018. A second large injection into this interval, Exp 2020, was conducted before a sand and barite plug was set at 3550 m (Dreesen and Nicholson, 1984) prior to Exp 2032. The plug was intended to cause the fracturing fluid to penetrate the few remaining exposed fractures while preventing extension of the sand-covered fractures. However, subsequent analysis of the Exp 2032 seismic data shows that the fracturing fluid flowed into the fractures that were supposed to be plugged where they intersected EE-2. Since plane 1A intersects EE-2 within 3 m of the top of the plug and at a small angle, it is very close to the open hole region of the wellbore. During Exp 2032, this resulted in a quick break down of the rock between the open hole and the fracture and subsequent flow into this plane. The close proximity of the three-point-determined plane to EE-2 thus provides an explanation for the observed flow into fractures that had previously been considered inaccessible to water.

Figure 1 shows a histogram of the number of seismic events occurring over 1 m intervals perpendicular to plane 1. There are two distinct peaks in the histogram suggesting the existence of two planes. The EE-2 temperature log taken after Exp 2018, projected onto the line normal to plane 1, is also presented in Figure 1. The log-to-histogram correlation shows that locations of temperature anomalies created by the fluid injection correspond fairly well with the locations where the peaks of the histogram occur. We consider each peak to be at the center of one plane. The correlation of temperature anomalies, which indicate zones where fluid was injected, with the microearthquake-defined planes further justifies our decision to split the original plane into two planes. In this case, the two planes

have the same orientation as was found for the original plane 1.

Seismic Intercepts in EE-3A

EE-3A intercepts the seismic regions of planes 2, 3B, 4A, 4B and 5A. Figure 2 shows a histogram of the total number of events associated with these planes projected parallel to each plane onto the EE-3A wellbore. Four distinct groups are apparent; those events associated with plane 3B, planes 5A and 4A, plane 4B, and plane 2.

The events associated with plane 4B and with planes 5A and 4A correlate best with the EE-3A injection zone observed on the post-2059 and post-2067 temperature logs, shown above the histogram in Figure 2.

Only minor borehole temperature anomalies are correlated with the intercepts of planes 2 and 3B. Exp 2032 seismic location density originally led us to conclude that the region of the plane 2 intercept was a highly developed portion of the reservoir. However, an injection into the region of EE-3A containing the intercept with plane 2, Exp 2061, resulted in more than 90% of the water being injected at the bottom of EE-3A, nearly 150 m farther downhole. We believe that the high normal stress on plane 2, due to its low dip, severely restricted flow into this plane and forced the water to enter and stimulate a deeper, higher-dip joint system not connected to the Exp 2032 reservoir. The lack of a major injection zone at the plane 3B intercept is not significant because this region was never isolated from the low pressure zones above (see section on reservoir structure) and stimulated.

In Table III, we summarize significant features of wellbore/plane intercepts in both the seismic and aseismic regions.

RESERVOIR STRUCTURE

In the previous section we described some of the correlations between seismically active regions of the planes and borehole injection zones. In Tables II and III we show evidence that all planes except plane 4 may be associated with regional faults or zones of weakness; i.e. the aseismic plane-wellbore intercepts have been correlated with wellbore breakout zones and/or low injection pressure zones.

The three point method was applied to locations of microearthquakes accompanying four fracturing experiments carried out in wellbores EE-2, EE-3 and EE-3A and it was found that the general orientation of plane 4 (strike N7°E, dip 67°E) is the only common orientation found for all the experiments (Fehler, 1987). Fehler showed that this orientation is close to the orientation of the plane with the largest ratio of shear to normal stress and is thus most likely to be the slip plane for earthquakes when the stress field is perturbed by fluid injections.

Figure 3 is a perspective view showing the 3 wellbores and the seismic regions of the planes. From Figure 3 it is evident that all of the seismic regions in planes 1 through 5 are interconnected, and that flow through the seismically active regions of the planes could have created the complete set of seismic planes forming the Exp 2032 reservoir.

In order to determine how the existence of various planes affects other planes, we examined the intersections of the seismic region of each plane with the seismic and aseismic regions of each remaining plane (Table IV). We conclude that both the seismically active and aseismic portions of plane 3A are major barriers to fracture extension in the reservoir. Four planes approach plane 3A; none penetrate it by more than a few meters. Plane 3A appears to be a low pressure leak-off zone which was seismic only in a small, 16,000 m^2, region connected directly to planes 1A, 1B, and 4C. Just 10 m below plane 3A lies plane 3B with a seismic region extending over 100,000 m^2. Plane 3B is penetrated by all the planes that stop at plane 3A. Plane 3B must open at a significantly higher pressure than 3A, indicating an abrupt transition in fracturing pressure in this region. An abrupt change in fracturing pressure with depth was found in the vicinity of the seismic portions of planes 3A and 3B (Kelkar et al., 1986). Figure 3 shows a possible direct flow path from EE-3A to EE-2 through plane 3B, though this has not been observed. Our inability to develop this connection can be explained by the existence of a low-pressure sink, plane 3A, which is well connected and in close proximity to plane 3B.

FLOW PATHS

Figure 4 is a schematic showing which planes intersect in their respective seismic regions and can thus be considered to be connected paths for fluid flow. The figure also shows which planes have wellbores intersecting their seismic regions. The thickness of line connecting the various features is qualitatively proportional to our assessment of the ability of water to flow from one feature to another, which is taken to be proportional to the length of the intersections in the seismic regions. In the discussion that follows, we assume that all fractures have low impedance and that the greatest resistance to flow occurs at the intersections between planes and at plane/wellbore intersections.

A relatively poor flow path from EE-3A to EE-2 is shown: plane 4A, the major injection fracture during Exp 2067, appears to be poorly connected to the main part of the reservoir, which helps explain the high flow impedance and water losses during this experiment (Hendron, 1987). If plane 4C, and possibly planes 3A and 3B, could be included in the flow path, the potential exists for a much larger reservoir than that determined from tracer tests conducted during Exp 2067, the last major injection into the reservoir. This inclusion may have occurred temporarily after a

gas-water mixture containing 5000 kg of nitrogen was injected down EE-3A during Exp 2067. The residence time for the nitrogen mixture was approximately 5 times longer than that measured for radioactive tracers injected before and after the nitrogen injection (Robinson et al., 1987), indicating that the low density mixture penetrated regions of the reservoir that tracer-containing water did not reach.

CONCLUSIONS

Comparisons of well log data with planes determined using the three point method show striking evidence that the seismic planes actually do exist. We have shown data to support our assertion that the planes defined by the three point method act as flow paths and/or barriers to plane extension. The planes defined by the three point method provide a consistent picture of a reservoir whose structure is in basic agreement with our present understanding of the regional stress field. This increases our confidence in using seismic data as a guide in determining fracture locations.

The possibility of drilling and completing a well that is connected to a fracture system induced by hydraulic stimulations in a nearby well can be enhanced by the application of the three point method to a high quality set of locations of microseismic events accompanying the injection. With the knowledge of fracture orientations gained prior to drilling, we can select targets and completion zones which provide desired reservoir size and impedance characteristics. Thus a major difficulty in creating a hot dry rock geothermal system can thus be overcome.

ACKNOWLEDGMENTS

The authors would like to thank Hugh Murphy and Jim Albright for their editorial suggestions, and John Paskiewicz and Ada DeAguero for assistance in manuscript preparation. We would also especially like to thank Andrew Maestas for many hours spent on the CAD/CAM generating 3-d plots. This work was supported by the U.S. Department of Energy. Data collection was also supported by the Governments of Japan and the Federal Republic of Germany through an International Energy Agency Agreement.

REFERENCES

Albright, J.N. and Hanold, R.H., (1986), "Seismic Mapping of Hydraulic Fractures Made in Basement Rocks," Proc. 2nd ERDA Enhanced Oil and Gas Recovery Symposium.

Dreesen, D.S., Nicholson, R.W., (1985), "Well Completion and Operations for MHP of Fenton Hill HDR Well EE-2," Geothermal Resources Council Transactions, Vol. 9, part II, p. 89.

Fehler, M., (1987), "Stress Control of Seismicity Patterns Observed During Hydraulic Fracturing Experiments Carried Out at the Fenton Hill Hot Dry Rock Geothermal Energy Site," Conference on Forced Fluid Flow in Fractured Rock Masses held in Gorky, France, (Proc. published by European Economic Commission in Brussels, Belgium).

Fehler, M., House, L. and Kaieda, H., (1987), "Determining Planes Along Which Earthquakes Occur: Method and Application to Earthquakes Accompanying Hydraulic Fracturing," in press, Journal of Geophysic Resources.

Hendron, R., "The U.S. Hot Dry Rock Project," 12th Workshop on Geothermal Reservoir Engineering, Stanford University, Stanford, CA, Jan. 21-22, 1987.

House, L., (1987), "Locating Microearthquakes Induced by Hydraulic Fracturing in Crystalline Rock," submitted.

House, L., Keppler, H. and Kaieda, H., (1985), "Seismic Studies of a Massive Hydraulic Fracturing Experiment," Trans. Geotherm. Res. Council, Vol. 9, part II, pp. 105-110.

Kelkar, S., Murphy, H. and Dash, Z., "Earth Stress Measurement in Deep Granitic Rock," 27th U.S. Symposium on Rock Mechanics, University of Alabama, June 23-25, 1986.

Lutz, T., (1986), "An Analysis of the Orientations of Large-Scale Crustal Structures: A Statistical Approach Based on Areal Distributions of Pointlike Features," Journal of Geophysic Resources, Vol. 1, pp. 421-434.

Murphy, H.D., (1982), "Enhanced Interpretation of Temperature Surveys Taken During Injection of Production," Journal of Petroleum Technology, June, p. 1313.

Pearson, C., (1981), "The Relationship Between Microseismicity and High Pore Pressure During Hydraulic Stimulation Experiments in Low Permeability Granitic Rocks," Journal of Geophysics, Vol. 86, pp. 7855-7864.

Robinson, B.A., Aguilar, R.G., Kanaori, Y., Trujillo, P.E., Counce, D.A., Birdsell, S.A., Matsunaga, I., "Geochemistry and Tracer Behavior During a Thirty Day Flow Test of the Fenton Hill HDR Reservoir," 12th Workshop on Geothermal Reservoir Engineering, Stanford University, Stanford, CA, Jan. 20-22, 1987.

Schomaker, V., Waser, J., Marsh, R.E. and Bergman, G., (1959), "To Fit a Plane or a Line to a Set of Points by Least Squares," Acta Cryst., Vol. 12, p. 600.

TABLE I

EXPERIMENT NUMBER	DATE	WELLBORE	OPENHOLE PARAMETERS: OPENHOLE INTERVAL* (m)	VOLUME INJECTED (m)	NOMINAL RATE (m /s)	NOMINAL PRESSURE (MPa)
2018	07/19-20/82	EE-2	3528-3656	910	0.0315	48.3
2020	10/06-07/82	EE-2	3528-3656	3,090	0.0928	46.9
2023	11/08/82	EE-3	3162-4084	150.#	0.0172	12.9
2032†	12/06-09/83	EE-2	3528-3550	21,200	0.1140	48.0
2042	05/15-19/84	EE-3	3420-3588	7,600	0.0265	41.4
2052	04/16-05/01/85	EE-2	3528-3550††	4,880	0.0050	14.5
2059**	05/27-28/85	EE-3A	3516-3719	1,590	0.0106	31.7
2061	06/29-07/02/85	EE-3A	3827-4017	5,230	0.0106	31.0
2062**	07/18-20/85	EE-3A	3651-3825	5,770	0.0106	35.9
2066	01/30-02/01/86	EE-3A	3755-3914	3,770	0.0199	46.9
2067**(ICFT)	05/19-06/18/86	EE-3A	3487-3750	37,000	0.0106 0.0185	26.9 30.3

*Actual injection intervals based on temperature surveys are specified in Table II.
#Only 31 very low magnitude earthquakes were recorded during this low pressure injection. At lower injection rates this region has remained virtually aseismic.
†This is the EE-2 MHF which is attributed with creating most of the reservoir flow system connecting EE-3A to ##-2.
††Injection also occurred at 3280 m where the 9-5/8" casing is damaged.
**Reservoir connection between EE-3A and EE-2 was demonstrated by flowing EE-2.

TABLE II. CORRELATION OF WELL LOG DATA TO CALCULATED WELLBORE INTERCEPTS OF PLANES LOCATED FOR EXPERIMENT 2032 (EE-2 MHF) EARTHQUAKE LOCATIONS

Plane	Description: Azimuth	Dip	Well (EE)	Well Interception: Depth (m)	Angle#	Seismic Region	Best Correlation to Temperature and caliper log data depth along wellbore (m)
1A	331	76E	2	3616	19.3	yes	Fig. 3, 38.5MPa lower major inj. zone 3590-3622
			2	2017	16.0	no	No logs
			3	2023	17.7	no	Borehole break out zone 1984-2013
1B	331	76E	2	3558	19.3	yes	Fig. 3, 38.5 MPa middle major inj. zone 3548-3569
			2	2081	13.1	no	No logs
			3	2817	7.7	no	Minor break out zone 2835-2847
			3	2090	10.9	no	None
			3A	3340	5.7	no	Borehole break out zone 3320-3322
2	268	27N	2	4107	42.8	no	none
			3A	3860	69.4	yes	Fig. 4, 38.5MPa temp. anomaly 3850-3865 Borehole break out zone 3857-3870
3A	151	67W	2	3263	45.2	no	none
			3	3104	54.0	no	12.9 MPa inj. zone 3060-3175
			3A	3159	32.6	no	Fig. 4, 9.5 MPa inj. zone 3066-3133
3B	151	67W	2	3281	44.8	yes	14.7 MPa inj. zone minor anomaly 3290-3350, 9-5/8" casing collapes below 3267
			3	3119	52.6	no	12.9 MPa inj. zone 3060-3175
			3A	3181	32.8	yes	Fig. 4, 9.5 MPa inj. zone 3066-3133
4A	006	67E	2	3056	9.6	no	14.7 MPa inj. zone major anomaly 2800-3170
			2	3838	6.3	no	none
			3A	3574	17.1	yes	Fig. 4, 31.5 MPa main ICFT inj. zone 3572-3603
4B	005	64E	3A	3692	19.5	yes	Fig. 4, 31.5 MPa lower ICFT inj. zone 3645-3658, Break out zones 3660-65 and 3591-3706
4C	008	67E	3A	3839	14.9	no	Fig. 4, 38.5 MPa temp. anomaly 3850-3865
5A	213	60W	2	3641	37.4	yes	Fig. 3, 38.5 MPa lowest minor anomaly 3618-3621
			3	3533	36.1	no	39.5 MPa inj. zone 3542-48 and 3567-68
			3A	3534	38.1	yes	Fig. 4, 31.5 MPa upper ICFT inj. zones 3493-3502 and 3520-3523
5B	214	56W	2	4030	48.3	no	none
			3	3979	50.6	no	no logs
			3A	3940	45.5	no	Fig. 4, 38.5 MPa Temp. anomaly 3923-3926

#Angle of wellbore to plane where low angle allows more deviation in well intersect depths due to plane location inaccuracies.

TABLE III
DISTINGUISHING FEATURES CORRELATED TO WELL INTERCEPT

Plane	Seismic Plane	Aseismic Extension of Plane
1 (A&B)	Main injection interval for injections into EE-2 preceeding Exp. 2032.*	Borehole breakout zones close to 3 of 4 intercepts with caliper logs.
2	Deep seismic target for EE-3A trajectory. Unable to inject into EE-3A intercept region to cause flow in EE-2 during Exp. 2061 or Exp 2066.	None
3 (A&B)	Intercepts are near temp. survey depths of 9.5 to 14.5 MPa (low pressure) injection intervals. Provided a seismic path from the reservoir to EE-3A backside which flowed 0.2 l/sec during Exp. 2057.	Intercepts are near temp. survey depths of 9.5 to 14.5 MPa (low pressure) injection intervals (Exps. 2032 & 2052)
4 (A,B&C)	Main injection interval during reservoir circulation from EE-3A to EE-2. (Exps. 2059, 2061 and 2067).	Plane 4A intersects EE-2 at a low pressure 14.5 MPa injection interval. (Exp. 2052)
	Plane 4C has no seismic intercepts.	
5 (A&B)	Plane 5A is an injection interval for experiments preceeding Exp 2032.* It was the only seismic plane connected to both EE-2 and EE-3A during Exp. 2067.	Plane 5A intercepts EE-3 near Exp. 2042 injection interval. No seismic planes with the same orientation were located using the 3 point method on the Exp. 2042 seismic data.
	Plane 5B has no seismic intercepts.	

*It is assumed that beyond the near wellbore area the planes were also tributaries for the injection fluid during Exp. 2032.

TABLE IV

PLANE	SEISMIC REGION: Seismic Planes Penetrating	SEISMIC REGION: Seismic Planes Approaching and Stopping	ASEISMIC REGION: Seismic Planes Penetrating	ASEISMIC REGION: Seismic Planes Approaching and Stopping
1A	3	1	2	0
1B	4	1	3	3
2	3	0	0	0
3A	0	3	0	4
3B	3	0	2	0
4A	3	1	6	0
4B	3	0	7	0
4C	4	1	5	2
5A	2	1	0	0
5B	2	0	1	0
TOTALS	27	8	26	9

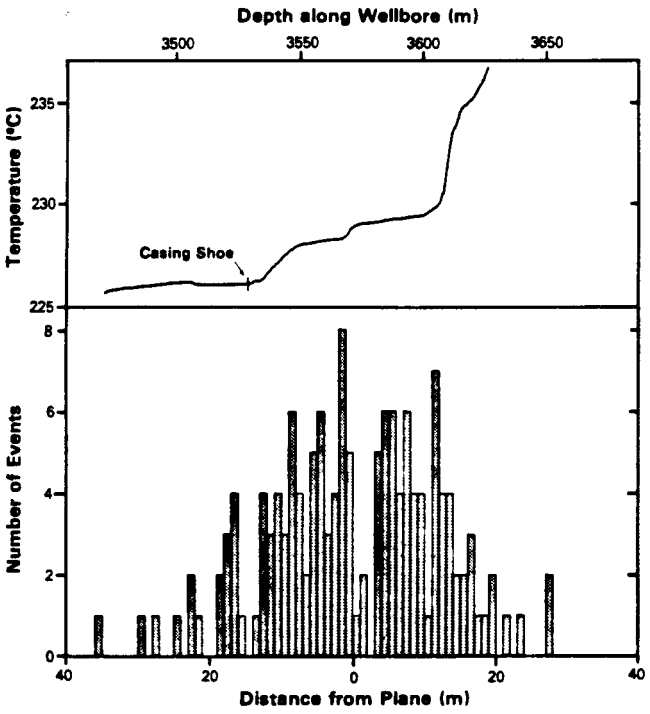

FIGURE 1. Histogram of the number of microearthquakes associated with plane 1 as a function of perpendicular distance from that plane. Above the histogram is a temperature log of wellbore EE-2 taken after Exp 2018 as projected onto the normal of plane 1. Since wellbore is not perpendicular to plane 1, scale for distance along wellbore is different than that for scale for distance perpendicular to plane.

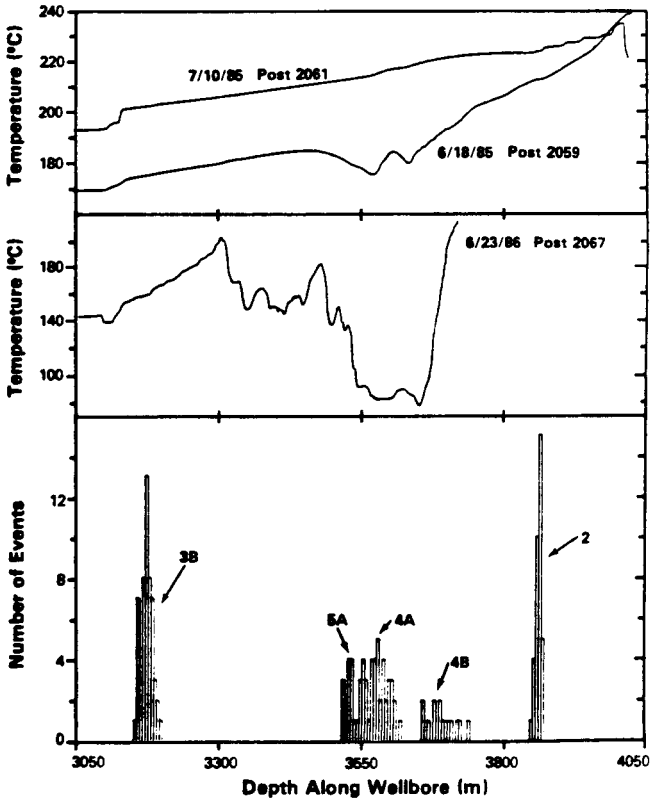

FIGURE 2. Histogram showing the number of seismic events projected parallel to each plane onto wellbore EE-3A. Only seismic events from planes intersecting the wellbore in the seismically active portions of the planes are shown. Temperature logs are shown for Exp 2061, Exp 2059 and Exp 2067.

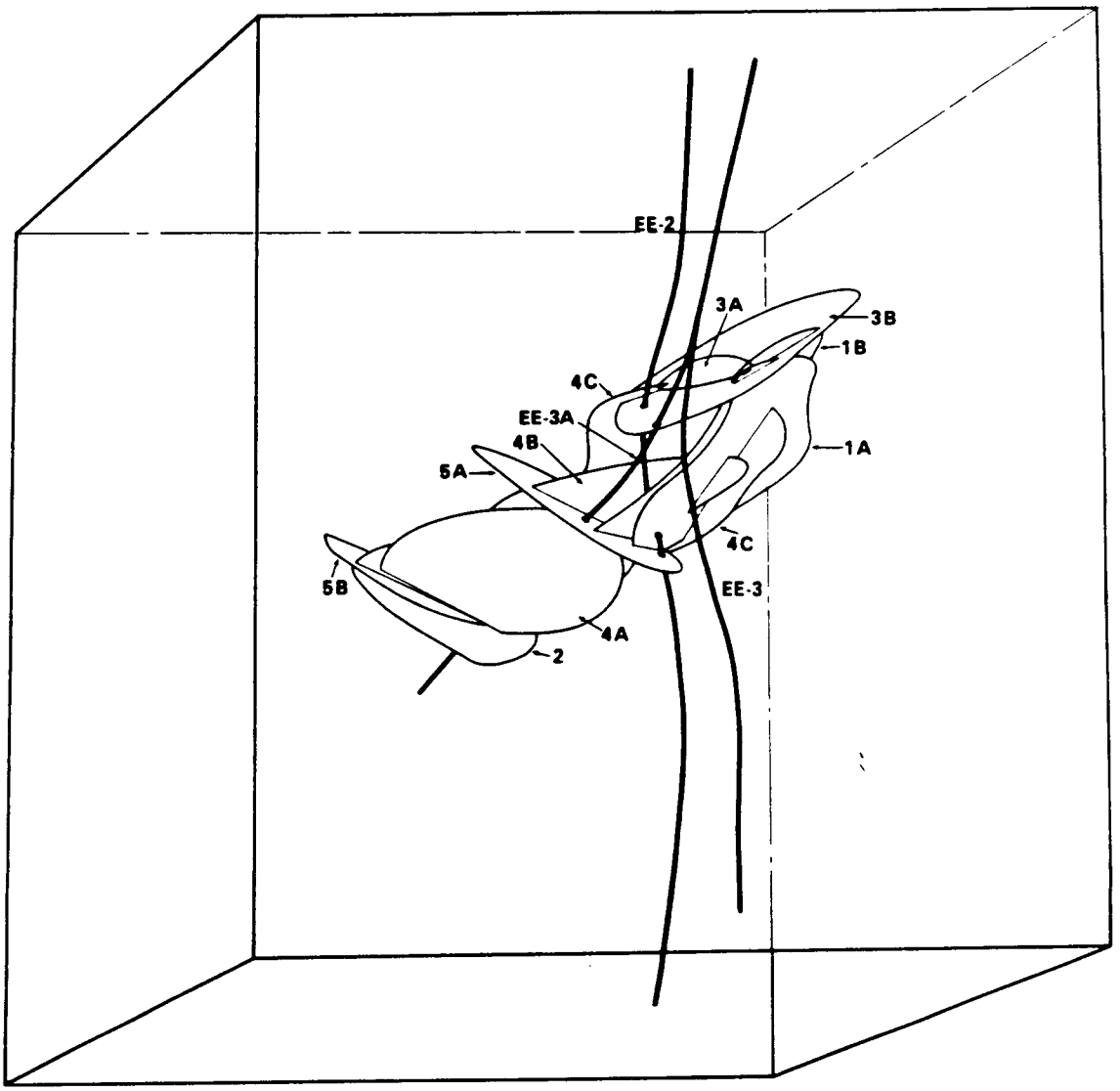

FIGURE 3. Perspective view of the three wellbores and the seismically active portions of the Exp 2032 planes identified using the three point method.

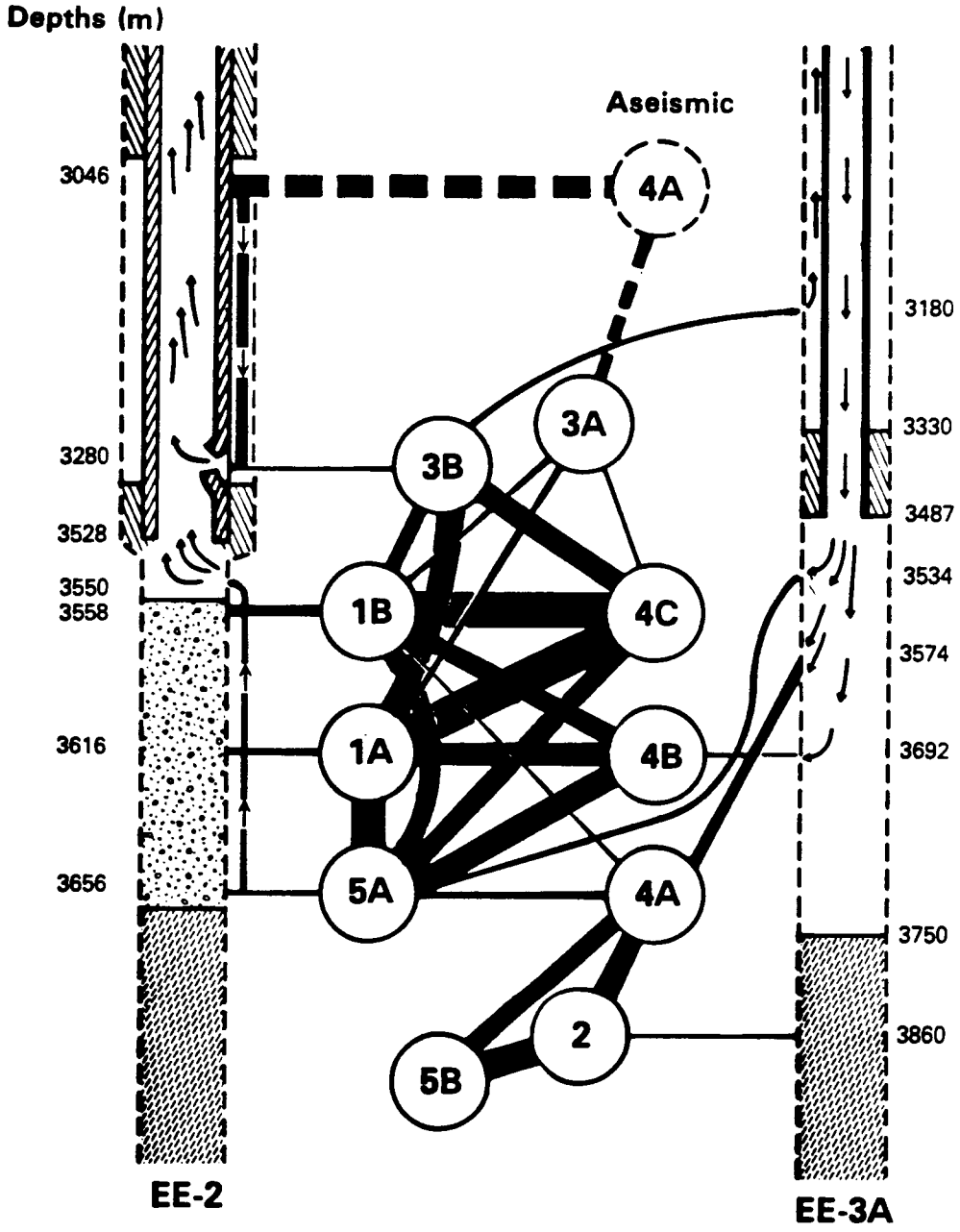

FIGURE 4. Schematic showing the interconnections between various seismic planes and wellbores. The thickness of lines connecting the various features is proportional to how easily fluid is estimated to flow between the features.